Astronomy
& **Astrophysics**

Energy and time-lag spectra of galactic black-hole X-ray sources in the low/hard state

P. Reig[1,3], N. D. Kylafis[2,3], and D. Giannios[2]

[1] G.A.C.E, ICMUV, Universitat de Valencia, 46071 Paterna-Valencia, Spain
[2] University of Crete, Physics Department, PO Box 2208, 710 03 Heraklion, Crete, Greece
[3] Foundation for Research and Technology-Hellas, 711 10 Heraklion, Crete, Greece

Abstract. Most, probably all, accreting binaries that are believed to contain a black-hole emit radio waves when they are in the low/hard state. Whenever this radio emission has been resolved, a jet-like structure has become apparent. We propose that Compton upscattering of low-energy photons in the jet can explain both the energy spectra and the time lags versus Fourier frequency observed in the low/hard state of black-hole systems. The soft photons originate in the inner part of the accretion disk. We have performed Monte Carlo simulations of Compton upscattering in a jet and have found that for a rather wide range of values of the parameters we can obtain power-law high-energy X-ray spectra with photon-number index in the range 1.5–2 and power-law time lags versus Fourier frequency with index ∼0.7. The black-hole source Cyg X-1 in the low/hard state is well described by our model.

Key words. accretion, accretion disks – black hole physics – radiation mechanisms: non-thermal – methods: statistical – X-rays: stars

1. Introduction

The continuum X-ray spectra of black-hole candidates are generally described by a soft component, normally modeled as a multi-colour black-body component (Mitsuda et al. 1984, but see Merloni et al. 2000) and a power-law hard tail, which is thought to be the result of Comptonization (see e.g. Sunyaev & Titarchuk 1980; Hua & Titarchuk 1995; Titarchuk et al. 1997; Psaltis 2001). Based upon the presence or absence of the soft component, the luminosity and spectral slope of the hard tail and the different shapes of the noise components in the power-density spectra, black-hole systems can be found in at least two spectral states: The low/hard and the high/soft states. In the low/hard state the soft component is weak or absent, whereas the hard tail extends to a few hundred keV in the form of a power law with photon-number index in the range 1.5–2. The power spectrum shows strong band-limited noise with a typical strength of 20%–50% rms and a break frequency below 1 Hz (van der Klis 1995).

There is growing evidence that all X-ray binaries harboring a black hole display radio emission when they are in the low/hard X-ray state (Fender 2001). Inverse Compton scattering by relativistic electrons in a jet has been proposed as a mechanism for the production of X-rays and γ-rays in Active Galactic Nuclei (Begelman & Sikora 1987; Bednarek et al. 1996; Harris & Krawczynski 2002) and X-ray binaries

(Band & Grindlay 1986; Levinson & Blandford 1996; Georganopoulos et al. 2002; Romero et al. 2002). The contribution of the synchrotron emission from the jet to the hard X-rays might also be significant (Markoff et al. 2001).

However, the Comptonization spectra cannot provide, by themselves, information about the geometry and the dynamics of the Comptonizing electrons, i.e., one can obtain similar energy spectra from rather different geometric configurations of the Comptonizing cloud (Titarchuk & Lyubarskij 1995). In addition to the energy spectra, time variability information is needed (Hua et al. 1999). Moreover, it has been observed (Miyamoto et al. 1988) that the phase lags (not the time lags) between the signals in two different X-ray energy bands are approximately constant with Fourier frequency. This cannot be explained if Comptonization takes place in a hot, uniform, low-density plasma. A clever way to bring into terms thermal Comptonization and timing behavior was to consider a stratified spherical medium with density inversely proportional to radius (Hua et al. 1997; Kazanas et al. 1997; Kazanas & Hua 1999; Hua et al. 1999).

Our proposal builds on the ideas presented in the above works. The relativistic electrons in the jet upscatter a fraction of the soft photons emitted by the inner part of the accretion disk and this produces the power-law energy spectrum. Power-law energy spectra with index in the range 1.5–2 are produced with reasonable values of the parameters describing the relativistic electrons in the jet. In addition, we show for the first time that, by considering a jet with density inversely proportional

Send offprint requests to: P. Reig, e-mail: `pablo@physics.uoc.gr`

to distance from the black hole, the nearly constant phase lags with Fourier frequency can be reproduced. For an alternative interpretation of time lags in black-hole candidates see Kotov et al. (2001).

2. The model

2.1. Characteristics of the jet

We consider the simplest model that we can think, which reproduces the energy spectrum and the time lags versus Fourier frequency that have been observed. The characteristics of the assumed jet are the following:

i) We assume the speed of the relativistic electrons in the jet to be constant.

ii) We assume that there exists a uniform magnetic field along the axis of the jet (taken to be the z axis) and that the velocity of the electrons $\boldsymbol{v}$ consists of two components: one parallel to the magnetic field $\boldsymbol{v}_\parallel$ and one perpendicular to it $\boldsymbol{v}_\perp$. In other words, the electrons in the jet are spiraling along the magnetic field lines. This upscattering mechanism is reminiscent of thermal Comptonization because the photons sample electrons with all possible velocities (Titarchuk & Lyubarskij 1995).

iii) We take the electron-density profile in the jet to be of the form

$$n_e(z) = n_0(z_0/z)^p \tag{1}$$

where z is the vertical distance from the black hole and p is a parameter (which in this work is taken equal to 1) and the parameters n_0 and z_0 are the electron density and height at the base of the jet respectively. If H is the height of the jet, then the Thomson optical depth along the axis of the jet is

$$\tau_\parallel = n_0\sigma_T z_0 \ln(H/z_0), \tag{2}$$

where σ_T is the Thomson cross section.

iv) Let πr^2 be the cross sectional area of the jet at height z. Then, from the continuity equation $\dot{M} = \pi r^2 m_p n_e(z) v_\parallel$ and $p = 1$, we obtain for the dependence of the radius r on height z that

$$r = \left(r_0^2 z/z_0\right)^{1/2}, \tag{3}$$

where $r_0 = (\dot{M}/\pi m_p n_0 v_\parallel)^{1/2}$ is the cross sectional radius of the jet at its base, $\dot{M}$ is the mass ejection rate and m_p is the proton mass. Our jet is therefore focused, in agreement with observations (Fender et al. 1999). The half Thomson optical depth of the jet at height z is

$$\tau_\perp(z) = n_0\sigma_T r_0(z_0/z)^{1/2}. \tag{4}$$

2.2. The Monte Carlo code

For our Monte Carlo code we follow Cashwell & Everett (1959) and Pozdnyakov et al. (1983). A similar code was described in previous work (Reig et al. 2001). The procedure is as follows:

Photons from a blackbody distribution of characteristic temperature T_{bb} are injected at the center of the base of the jet with an upward isotropic distribution. As the photons travel

through the medium, they experience Compton scatterings with the spiraling electrons. If the effective optical depth that they encounter is small ($\lesssim 1$), the majority of the input photons escape unscattered. If the effective optical depth is moderate, then the photons random walk through the medium prior to escape and on average gain energy from the circular motion (i.e., $\boldsymbol{v}_\perp$) of the electrons. Such Comptonization can occur everywhere in the jet.

If the defining parameters of a photon (position, direction, energy and weight) at each stage of its flight are computed, then we can determine the spectrum of the radiation emerging from the scattering medium and the time delay of each escaping photon. The optical depth to electron scattering, the frequency shift and the new direction of the photons after scattering are computed using the corresponding relativistic expressions. The extra time of flight of each photon outside the jet is taken into account in order to bring in step all the photons escaping in a given direction.

3. Parameter values

The high-energy X-ray spectra of black-hole candidates in the low/hard state are characterized by a power law with photon-number spectral index in the range $1.5 \lesssim \Gamma \lesssim 2$ and a high-energy cutoff in the range $150 \lesssim E_{cut} \lesssim 300$ keV (see e.g. Tanaka & Shibazaki 1996). In addition, the soft thermal component, so prominent in the high/soft state and interpreted as radiation from a cold accretion disk, never totally disappears in the low/hard state. There is evidence for a soft excess with blackbody temperatures $kT_{bb} \sim 0.1-0.3$ keV (Balucińska-Church et al. 1995; Wilms et al. 1999). In particular, for Cyg X–1 these parameters are $kT_{bb} = 0.13$ keV, $\Gamma = 1.6$, $E_{cut} = 160$ keV (Dove et al. 1998; di Salvo et al. 2001). Thus we have considered a blackbody function with $kT_{bb} = 0.2$ keV as the input source of soft photons in all the calculations presented in this work. Our conclusions are unchanged for $0.1 \lesssim kT_{bb} \lesssim 0.3$ keV.

Observed time lags of the order of a fraction of a second, if interpreted as light-travel times, require a height H of the jet at least of the order of 10^{10} cm. In our calculations we have taken $H = 2 \times 10^5 r_g$, where $r_g = (GM/R)^{1/2}$ is the gravitational radius of a black hole of mass M and horizon radius R. Thus, for a 10 $M_\odot$ black hole $H = 3 \times 10^{11}$ cm.

Both E_{cut} and Γ depend on the velocity of the electrons in the Comptonizing medium. In order to produce spectra similar to the ones observed, we restricted the values of v and $v_\perp$ to the ranges $0.7c \lesssim v \lesssim 0.9c$ and $0.3c \lesssim v_\perp \lesssim 0.5c$. When another parameter in our calculations is varied, we take $v = 0.85c$ and $v_\perp = 0.4c$.

Another parameter of our model that affects the slope of the resulting energy spectra is the width of the jet, since in a too narrow a jet too few photons are upscattered. The base of the jet was fixed at a distance of $z_0 = 20r_g$ from the black hole, whereas r_0 was varied in the range $75r_g \lesssim r_0 \lesssim 300r_g$. When another parameter in our calculations is varied, we take $r_0 = 200r_g$.

In order to have enough scatterings to produce the desired power-law energy spectra, we have taken $3 \lesssim \tau_\parallel \lesssim 15$,
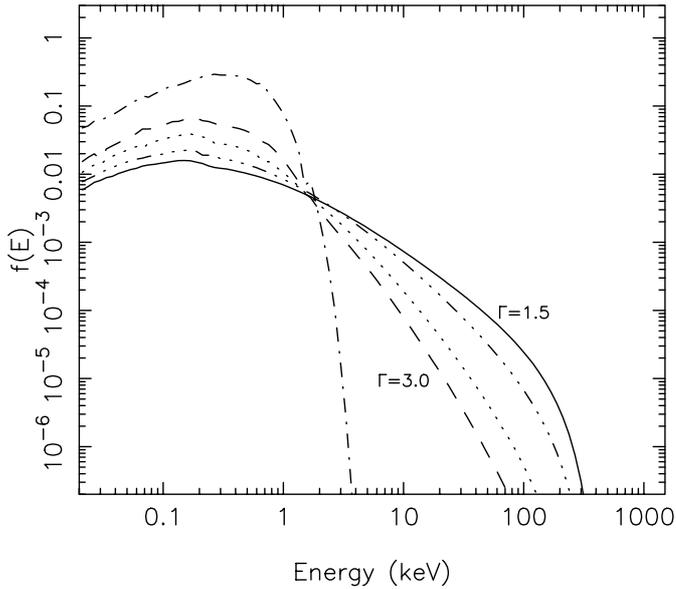
Fig. 1. Emergent photon-number spectra from our Monte Carlo simulations. The plotted lines correspond to the values $\tau_\parallel = 0$ (dot-dashed), 3 (dashed), 5 (dotted), 10 (dot-dot-dot-dashed) and 15 (solid) of the vertical optical depth.

Fig. 2. Photon-number spectral index as a function of **a)** optical depth $\tau_\parallel$, **b)** perpendicular component of the electron velocity $v_\perp$, **c)** base radius of the jet r_0 and **d)** escaping angle θ with respect to the z axis.

with fixed value $\tau_\parallel = 10$ when another parameter is varied. Note that the effective optical depth that the emitted photons see is significantly less than this due to the high velocity of the electrons in the jet.

Finally, given the high values of $v_\parallel$ invoked in our model, we expect an angular dependence of the power-law X-ray spectra. From observations of Galactic microquasars we know that the angle between the observational direction and the axis of the jet lies in the range $70°-85°$ (Mirabel & Rodríguez 1999). When a parameter is varied in our model, we restrict ourselves to photons recorded in the range $0.1 < \cos\theta < 0.3$ or $84° > \theta > 72°$, where θ is the angle between the direction of motion of the jet and the line of sight.
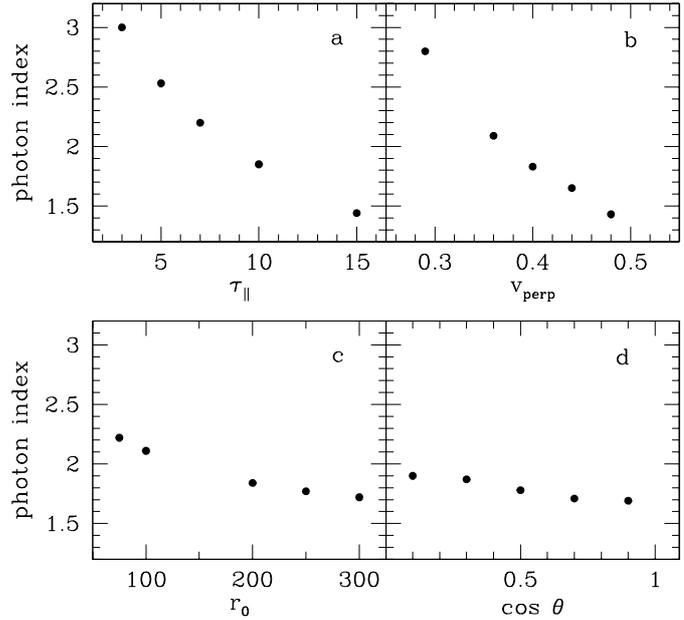
A thorough study of the dependence of the energy and time-lag spectra on the different parameters (including different density laws) will be presented in a forthcoming paper (Giannios et al., in preparation).

4. Results and discussion

In order to compute the energy spectra and the light curves we binned the energy of the escaping photons, their travel time and their direction cosine with respect to the axis of the jet.

4.1. Energy spectra

Figure 1 shows the emerging spectra from the jet for the fixed values of the parameters discussed in Sect. 3 and various optical depths $\tau_\parallel = 0$, 3, 5, 10 and 15. All curves are normalized to unity. The curve corresponding to $\tau_\parallel = 0$ gives the input blackbody spectrum. All spectra exhibit a soft, thermal-type component and a hard, power-law type component with a high-energy cutoff.

Figures 2a–d show the photon-number spectral index Γ of the hard power-law tail in the energy range 10–100 keV as a function of a) the optical depth $\tau_\parallel$, b) the perpendicular component of the electron velocity $v_\perp$, c) the radius of the jet r_0 at its base and d) the escaping angle θ with respect to the z axis. For intermediate optical depths, the photon-number index lies in the interval $\sim 1.5-2$, which is similar to that observed in the low/hard state of black-hole candidates (Tanaka & Shibazaki 1996). The thicker the medium the flatter the spectrum. The component $v_\perp$ must be a significant fraction of the total speed of the electrons in order to have $1.5 \lesssim \Gamma \lesssim 2$. The larger $v_\perp$ the flatter the spectrum. For the other two parameters, acceptable values of the spectral index are obtained over a broad range of radii r_0 and escaping angles θ.

4.2. Time lags

The time of flight of all escaping photons was recorded in 8192 time bins of duration 1/128 s each. This time was computed by adding up the path lengths traveled by each photon and dividing by the speed of light. Then we considered the light curves of two energy bands: 2–5 keV and 14–45 keV. Following Vaughan & Nowak (1997), we computed the phase lag and through it the time lag between the two energy bands as a function of Fourier frequency.

Figure 3 shows the time lag as a function of Fourier frequency for the fixed values of the parameters (Sect. 3). The data points have been logarithmically rebinned for clarity. The time-lag spectrum is roughly represented by a power law $\nu^{-\beta}$ with index $\beta = 0.7$ in the frequency range 0.3–30 Hz, in excellent agreement with the results of Cyg X-1 (Nowak et al. 1999).

Letter to the Editor
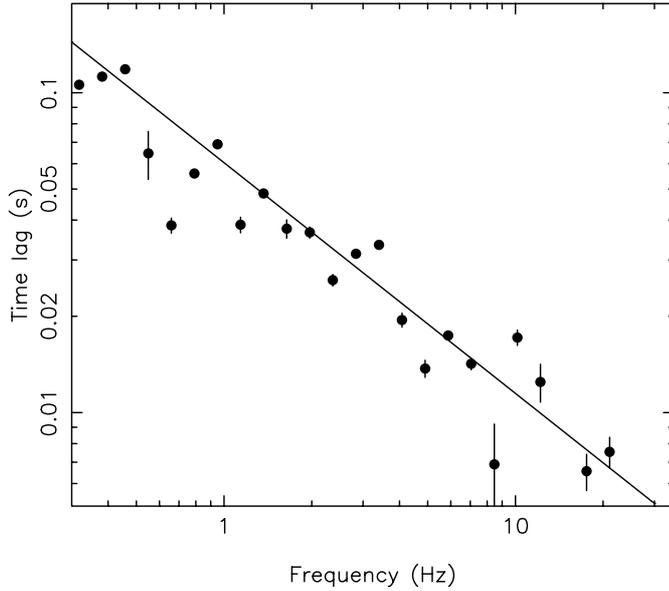
Fig. 3. Computed time lag as a function of Fourier frequency when the fixed values of the parameters are used. Positive lags indicate that hard photons lag soft photons. The best-fit power law is $\nu^{-0.7}$.

4.3. Energetics

For the fixed values of the parameters $\tau_\parallel = 10$, $v = 0.85c$, $v_\perp = 0.4c$, $z_0 = 20r_g$, $r_0 = 200r_g$ it is straightforward to show that the available kinetic luminosity in the jet is much larger than the X-ray luminosity of black-hole sources in the low/hard state. Thus, the soft photons steal only a small fraction of the energy in the jet with their upscattering.

5. Conclusion

We have shown that Compton upscattering of low-energy photons in a jet can explain both the energy and time-lag spectra in black-hole X-ray sources in the low/hard state. For reasonable values of the model parameters we are able to reproduce the energy and time-lag spectra of Cyg X-1 in the low/hard state.

References

Band, D., & Grindlay, J. E. 1986, ApJ, 311, 595
Balucińska-Church, M., Belloni, T., Church, M. J., & Hasinger, G. 1995, A&A, 302, L5
Bednarek, W., Kirk, J. G., & Mastichiadis, A. 1996, A&AS, 120, 571
Begelman, M. C., & Sikora, M. 1987, ApJ, 322, 650
Cashwell, E. D., & Everett, C. J. 1959, A Practical Manual on the Monte Carlo Method for Random Walk Problems (Oxford: Pergamon)
di Salvo, T., Done, C., Zycki, P. T., Burderi, L., & Robba, N. R. 2001, ApJ, 547, 1024
Dove, J. B., Wilms, J., Nowak, M. A., Vaughan, B. A., & Begelman, M. C. 1998, MNRAS, 298, 729
Fender, R., Garrington, S. T., McKay, D. J., et al. 1999, MNRAS, 304, 865
Fender, R. 2001, MNRAS, 322, 31
Georganopoulos, M., Aharonian, F. A., & Kirk, J. G. 2002, A&A, 388, L25
Harris, D. E., & Krawczynski, H. 2002, ApJ, 565, 244
Hua, X., & Titarchuk, L. 1995, ApJ, 449, 188
Hua, X., Kazanas, D., & Titarchuk, L. 1997, ApJ, 482, L57
Hua, X., Kazanas, D., & Cui, W. 1999, ApJ, 512, 793
Kazanas, D., Hua, X., & Titarchuk, L. 1997, ApJ, 480, 735
Kazanas, D., & Hua, X. 1999, ApJ, 519, 750
Kotov, O., Churazov, E., & Gilfanov, M. 2001, MNRAS, 327, 799
Levinson, A., & Blandford, R. 1996, ApJ, 456, L29
Markoff, S., Falcke, H., & Fender, R. 2001, A&A, 372, L25
Merloni, A., Fabian, A., & Ross, R. 2000, MNRAS, 313, 193
Mirabel, I. F., & Rodríguez, L. F. 1999, ARA&A, 37, 409
Mitsuda, K., Inoue, H., Koyama, K., et al. 1984, PASJ, 36, 741
Miyamoto, S., Kitamoto, S., Mitsuda, K., & Dotani, T. 1988, Nature, 336, 450
Nowak, M. A., Vaughan, B. A., Wilms, J., Dove, J. B., & Begelman, M. C. 1999, ApJ, 510, 874
Pozdnyakov, L. A., Sobol, I. M., & Sunyaev, R. A. 1983, Astrophys. & Space Phys. Rev., 2, 189
Psaltis, D. 2001, ApJ, 555, 786
Reig, P., Kylafis, N. D., & Spruit, H. C. 2001, A&A, 375, 155
Romero, G. E., Kaufman Bernadó, M. M., & Mirabel, F. 2002, A&A, 393, L61
Sunyaev, R. A., & Titarchuk, L. G. 1980, A&A, 86, 121
Tanaka, Y., & Shibazaki, N. 1996, ARA&A, 34, 607
Titarchuk, L., & Lyubarskij, Y. 1995, ApJ, 450, 876
Titarchuk, L., Mastichiadis, A., & Kylafis, N. D. 1997, ApJ, 487, 834
van der Klis, M. 1995, in The lives of neutron stars, ed. M. A. Alpar, Ü. Kiziloglu, & J. van Paradijs, NATO ASI Series C450 (Kluwer Academic Publishers)
Vaughan, B. A., & Nowak, M. A., ApJ, 474, L43
Wilms, J., Nowak, M. A., Dove, J. B., Fender, R. P., & di Matteo, T. 1999, ApJ, 522, 460